Emission Spectra of Group 13 Metal Atoms and Indium Hydrides in Solid H_2 and D_2

Xuefeng Wang, Bret Wolfe,† and Lester Andrews*

University of Virginia, Department of Chemistry, McCormick Road, P.O. Box 400319, Charlottesville, Virginia 22904-4319

Received: February 4, 2004; In Final Form: March 4, 2004

Infrared spectra of solid hydrogen (deuterium) samples co-deposited at 3.5 K with laser-ablated Al, Ga, In, and Tl atoms reveal infrared absorptions for the MH [MD] molecules. Irradiation at 193 nm increases MH_2 and MH_3 [MD_2 and MD_3] absorptions and produces emission spectra for the metal atoms except for Al and phosphorescence spectra for the InH [InD] molecules. Unreacted metal emission bands are blue-shifted from the gas phase more by solid D_2 than by solid H_2. However, the emission yield for InD is much higher in solid D_2 than for InH in solid H_2, which suggests a higher nonradiative relaxation rate in solid H_2 than in solid D_2 owing to the larger zero-point motion.

Introduction

Solid molecular hydrogens (H_2 and D_2) have been investigated extensively for several decades.[1] These low-molecular-weight solids are finding increasing use as media for investigating infrared spectra of new hydride species.[2−13] As far as vibrational spectra are concerned, most guest frequencies in solid H_2 and D_2 appear between neon and argon matrix values,[6−12] although small differences in frequencies do exist for common molecules in solid *n*-H_2, *p*-H_2, and *n*-D_2.[7]

In the past year we have co-deposited laser-ablated metal atoms with normal H_2 and D_2 at 3.5 K and trapped metal hydride [deuteride] reaction products for infrared spectroscopic investigation.[6−11] Deuterium was used as a matrix to trap or react metal atoms before hydrogen[9,11,14] because the freezing point of D_2 (18.7 K) is higher than that for H_2 (13.9 K),[1] and accordingly solid D_2 is a more robust matrix in the 4 K range typically employed for these experiments. We have noticed several important differences. First, the lower freezing point of H_2 reduces the condensation rate and efficiency, and makes the trapping of reactive species more difficult in solid H_2. Second, deuterium is a more rigid solid at 3.5 K, and reactions of trapped species can be observed on annealing up to 10 K, but solid hydrogen can be handled only up to 7 K before evaporation. Third, H_2 is more reactive than D_2, and metal hydride band intensities are typically 4 to 5 times higher than metal deuteride band intensities whereas the relative absolute intensities are a factor of almost two. Other differences between solid H_2 and D_2 have been described including NMR properties.[1,15]

Emission spectra from solid H_2 and D_2 have been reported by two groups using proton or electron irradiation as an excitation source. Brooks described the $^4S \rightarrow {}^2D$ emission from N atoms in solid H_2 (523.36 nm) and D_2 (523.37 nm) as red-shifted from the gas-phase position, and the $A\ ^3\Delta_u \rightarrow X\ ^3\Sigma_g^+$ emission of O_2 in solid H_2 and D_2 (33 990 ± 100 cm^{-1}) red-shifted 330 ± 100 cm^{-1} from the gas-phase value and concluded that differences between matrixes lie within experimental error.[16] Schou et al. report bound-free rare-gas hydride emissions near gas-phase values and note the intensity of XeH in solid H_2 was about a factor of 4 lower than that for XeD in solid D_2.[17]

Laser-induced fluorescence (LIF) from solid hydrogen (actually DT) was first reported by the Livermore group, who investigated excitations and emission of trapped excess electrons.[18] Such electron "bubbles" have received extensive further study using Rydberg excitation of trapped NO as a source of electrons.[19−21] Further LIF investigations of trapped O_2 and O atoms find small red shifts in solid D_2.[22,23] These and thermoluminescence studies show that O atoms are stable in solid hydrogen.[24] Finally, the first Group 13 member, B, shows a large blue shift in atomic absorption in solid H_2 and a larger blue shift in solid D_2, but the emission in solid H_2 is almost the same as that found in the gas phase.[25] This observation is explained using the "electron bubble" model[18−21] involving a repulsive interaction with the matrix cage, followed by cage expansion, then electronic emission before the cage can relax.[25]

In the course of recent investigations on Group 13 metal atom reactions with H_2 and D_2, we employed 193 nm laser irradiation to initiate the metal atom−hydrogen molecule reaction.[26−29] We noticed a very strong red glow from In/D_2 samples and a weak indigo emission from In/H_2 matrixes.[28] The characterization of these emissions forms the basis of the present comparative low-resolution investigation using solid H_2 and D_2 hosts for emission spectroscopy of the InH and InD molecules, and the Ga, In, and Tl atoms. We find novel and interesting matrix effects for solid H_2 and D_2.

Experimental Section

The laser-ablated metal matrix-isolation experiment for hydrogen has been described previously.[6−9,30] Emission spectra were recorded on an Ocean Optics USB 2000 optical fiber spectrometer (400 nm blaze grating, 2 nm resolution) of the 1064 nm (1−4 mJ/pulse, 10 Hz, focused) induced emission plume from the metal targets and from the solid matrix samples using 193 nm excitation (2−6 mJ/pulse, 10 Hz not focused) from an Optex (Lambda Physik) argon fluoride laser. A Sony ILX511 linear CCD array detector with 3 ms response was employed so shorter photophysical phenomena cannot be observed here. Each spectrum was integrated for 4 s to enhance signal-to-noise. Figure 1 shows the experimental arrangement.

* Corresponding author. E-mail: lsa@virginia.edu.
† Guest worker from the Department of Environmental Sciences, University of Virginia, Charlottesville, VA 22904-4123.

10.1021/jp0494887 CCC: $27.50
Published on Web 05/21/2004

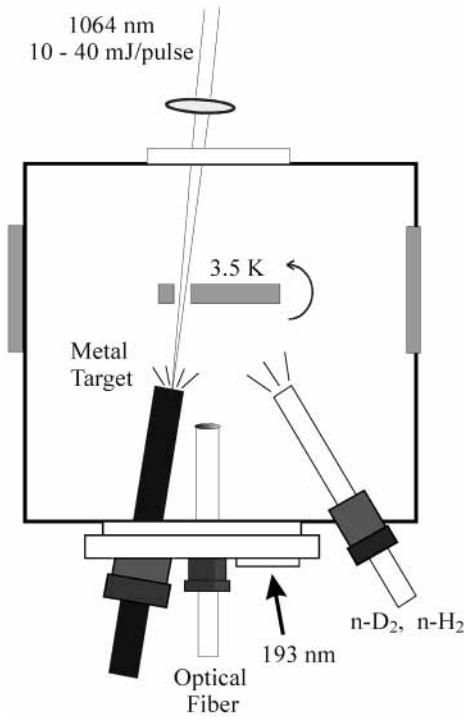

Figure 1. Schematic diagram of apparatus for laser-ablation matrix-isolation experiment with 193 nm excitation for emission spectroscopy of trapped species.

Sample emission was focused onto the optical fiber using a lens (12.7 mm dia, 25 mm f.l.) collection system sealed to fit inside of our vacuum chamber. Comparable weaker spectra were observed with the lens system outside of the vacuum chamber. Finally, experiments were done with In and enriched *p*-H_2 and *o*-D_2 prepared over catalyst in a copper tube immersed in cold gas over liquid helium.

Results

Emission spectra will be presented for Ga, In, and Tl and hydrogen systems in turn. No metal emission was observed for Al in solid H_2 using 193 nm excitation, as the reaction to give aluminum hydrides was complete.[26]

Ga. Laser-ablated Ga was co-deposited with pure hydrogen, and GaH infrared absorptions were observed at 1529.8 and 1516.9 cm^{-1} ($A = 0.02$) site-split by the hydrogen matrix, and weak GaH_2 absorptions were found at 1814.9 and 1746.1 cm^{-1}.[27] Irradiation at 193 nm for 10 min reduced the GaH absorptions, markedly increased the GaH_2 bands, and produced a strong GaH_3 band at 1928.7 cm^{-1}. An emission spectrum from the 1064 nm laser ablation plume is shown in Figure 2(a): Strong Ga and weaker Ga^+ emissions are observed at 403.4, 417.3 nm and at 296.4, 337.5, 426.6, 541.8 and 633.4 nm.[23,24] The Ga^+ emission intensities increased markedly relative to Ga with higher laser energies. The emission spectrum induced by 193 nm excitation of the solid H_2 sample is illustrated in Figure 2(b): a weak spin−orbit Ga doublet was observed at 400.0 and 413.5 nm with 1:2 relative intensity and blue-shifted 220 ± 20 cm^{-1} from the gas-phase atomic $^2S_{1/2} \rightarrow {}^2P_{1/2,3/2}$ band positions.[31] The broad 344 and 516 nm emissions remained on the cold window after evaporating the H_2 matrix, so they are probably due to aggregate species. However, the new 288 nm emission disappeared with the Ga doublet on annealing.

In like manner, laser-ablated Ga was co-deposited with pure deuterium, and GaD absorptions were found at 1104.2 and 1091.5 cm^{-1} and weak GaD_2 bands at 1315.5 and 1259.2 cm^{-1}.

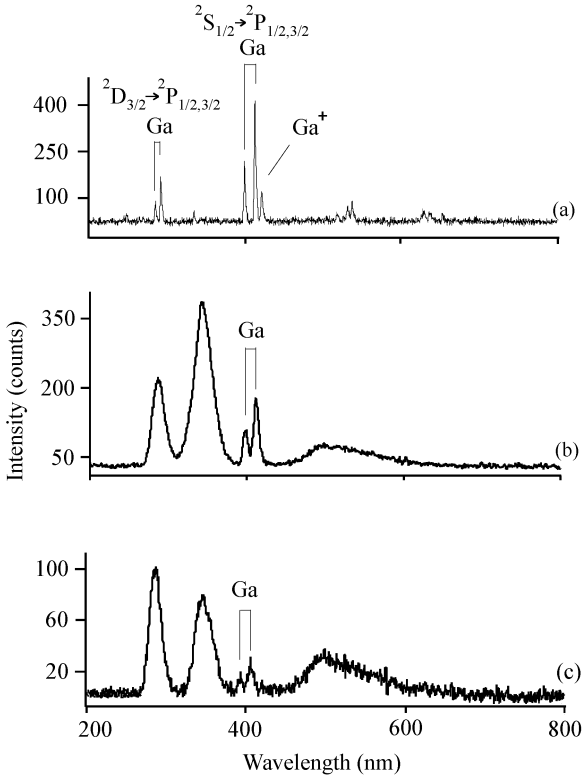

Figure 2. Emission spectra from gallium experiments. (a) Spectra of 1064-nm ablation plume over Ga target, (b) spectra of 193-nm induced emission from Ga/H_2 sample, and (c) spectra of 193-nm induced emission from Ga/D_2 sample.

TABLE 1: Resonance Spin−Orbit Emission Doublets (cm^{-1}) for Ga, In, and Tl in the Gas Phase, Solid H_2, and Solid D_2

metal	medium[a,b]	$^2S_{1/2} \rightarrow {}^2P_{1/2}$	$^2S_{1/2} \rightarrow {}^2P_{3/2}$
Ga	gas	24 789	23 963
	H_2	25 000	24 180
	D_2	25 380	24 560
	H_2 shift	210 ± 20	220 ± 20
	D_2 shift	590 ± 20	600 ± 20
In	gas	24 373	22 160
	H_2	24 680	22 480
	D_2	25 120	22 920
	H_2 shift	310 ± 20	320 ± 20
	D_2 shift	750 ± 20	760 ± 20
Tl	gas	26 478	18 685
	H_2	26 690	19 000
	D_2	27 140	19 460
	H_2 shift	210 ± 20	315 ± 20
	D_2 shift	660 ± 20	775 ± 20

[a] Gas phase from ref 23. [b] Solid H_2 and D_2, this work, accuracy ±20 cm^{-1}.

Irradiation at 193 nm for 10 min slightly increased GaD and markedly increased GaD_2 absorptions while producing a strong 1391.1 cm^{-1} GaD_3 band.[27] The emission spectrum from the solid D_2 sample is shown in Figure 2(c): The weak spin−orbit Ga doublet was observed at 394.0 and 407.1 nm and blue-shifted 600 ± 20 cm^{-1} from the gas-phase positions. These observations are summarized in Table 1. The same broad 344 and 516 nm emissions were observed, but the new feature shifted to 286 nm and disappeared with the Ga doublet on annealing.

In. Indium was co-deposited with pure hydrogen using 1064 nm ablation, and the emission spectrum of the ablation plume is shown in Figure 3(a): the strong purple emission in the laser-ablation plume from the target surface was dominated by the strong spin−orbit split indium $^2S_{1/2} \rightarrow {}^2P_{1/2,\,3/2}$ doublet at 410.3

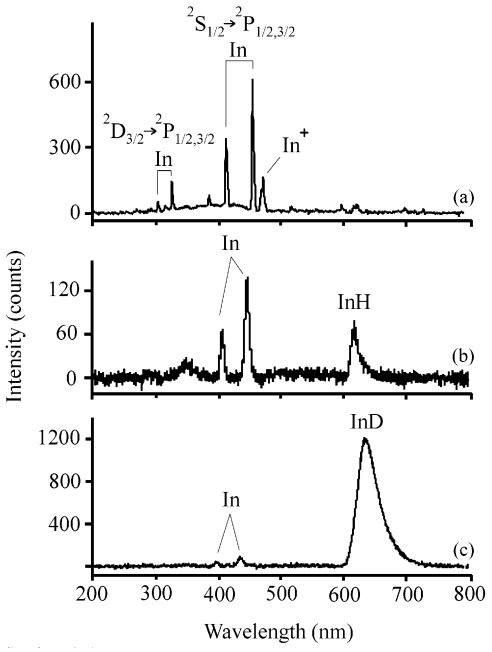

Figure 3. Emission spectra from indium experiments. (a) Spectra of 1064-nm ablation plume over In target, (b) spectra of 193-nm induced emission from In/H_2 sample, and (c) spectra of 193-nm induced emission from In/D_2 sample.

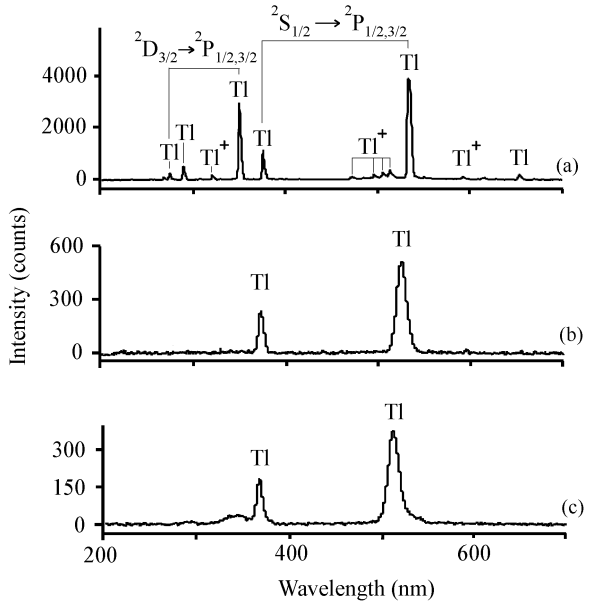

Figure 4. Emission spectra from thallium experiments. (a) Spectra of 1064-nm ablation plume over Tl target, (b) spectra of 193-nm induced emission from Tl/H_2 sample, and (c) spectra of 193-nm induced emission from Tl/D_2 sample.

and 451.3 nm, which was used to calibrate the spectrometer.[31] The weaker indium $^2D_{3/2} \rightarrow {}^2P_{1/2,\,3/2}$ doublet at 303.9 and 325.6 nm and In^+ lines at 383.5 and 468.5 nm were also observed:[31,32] the In^+ emission intensities were particularly sensitive to laser energy. The infrared spectrum revealed InH at 1407.9, 1393.4 cm^{-1} and weak InH_2 absorptions.[28] Irradiation at 193 nm increased InH, markedly increased InH_2, and produced InH_3, as described previously,[28] and produced a sharp red emission at 615.0 ± 0.3 nm and sharp 405.2 and 444.8 ± 0.3 nm lines. Additional experiments were done in 98% *p*-H_2, and the signals were measured at 405.4 ± 0.3, 445.5 ± 0.3, and 615 ± 1 nm.

Similar experiments with In and pure deuterium gave InD at 1011.3 and 999.7 cm^{-1} and weak InD_2 infrared bands.[28] Subsequent irradiation at 193 nm also increased InD, markedly increased InD_2, and produced InD_3. In contrast, a very strong broad red emission was observed at 636 ± 1 nm (even with the naked eye), and sharp lines were observed at 398.1 and 436.2 ± 0.3 nm. The absolute intensities of the sharp atomic emission doublets are about the same in the two solid molecular hydrogens. Additional experiments were done with 98% *o*-D_2, and the signals were measured at 398.8 and 436.6 ± 0.3 nm and at 626 ± 1 nm. The 193 nm laser pulse rate was varied from 1 to 20 Hz, which enabled us to estimate the strong emission lifetime of about 0.1 s in solid D_2: at 1 and 2 Hz the emission was clearly off more than on, at 3 Hz the emission was equally on, off, on, off, and at 4 and 5 Hz the emission was on more than off, and at 10 Hz, the emission appeared continuous to the naked eye.

Tl. Emission spectra were recorded from the 1064 nm laser-generated plume above the target surface during ablation-deposition. The strong Tl atomic spin−orbit doublets[31] were observed at 377.7, 535.2 nm and at 276.9, 353.0 nm as shown in Figure 4. In addition, weaker Tl^+ lines were found at 329.1, 507.7, 515.4, and 595.0 nm.[32]

Laser-ablated Tl co-deposited with pure hydrogen produced TlH at 1311.3 cm^{-1} and weak TlH_2 absorptions at 1519.9 and 1390.2 cm^{-1}.[29] Irradiation at 193 nm for 5 min increased TlH, markedly increased TlH_2, produced a weak TlH_3 absorption at 1748.4 cm^{-1}, and induced the atomic emission spectrum in Figure 4(b) containing 374.7 and 526.2 nm lines. In a similar deuterium experiment with Tl, the TlD absorption was observed at 939.9 cm^{-1} and very weak TlD_2 bands appeared at 1098.8 and 1007.6 cm^{-1}.[29] Irradiation at 193 nm for 10 min increased TlD 3-fold, markedly increased TlD_2, produced a weak TlD_3 band at 1254.4 cm^{-1}, and induced the 368.5 and 513.8 nm atomic emission shown in Figure 4(c).

Discussion

Two interesting hydrogen and deuterium matrix observations will be described in turn, namely, the blue-shifted atomic resonance emissions, and the phosphorescence of InH and InD.

Atomic Emissions. The atomic emissions observed in the laser ablation plume, Figures 2, 3, and 4, spectra (a), all show that metal atoms are ablated and excited and serve as a calibration[31] for 193 nm induced emission spectra from solid molecular hydrogens.

The matrix absorption spectrum at 193 nm (6.42 eV) has only been recorded for In in solid argon and neon.[33] Both of these matrixes reveal broad 6.0−6.8 eV absorptions, but their assignment is not straightforward. It is clear, however, from our work that 193 nm radiation activates the further reaction of In and InH in solid hydrogen. Hence, it is no surprise to observe emissions from both InH and atomic In in solid hydrogen.

The two emission bands in Figures 2, 3, and 4, spectra (b) and (c), are assigned on the basis of 1:2 relative intensity and proximity with the corresponding gas-phase emissions[31] to the spin−orbit $^2S_{1/2} \rightarrow {}^2P_{1/2,\,3/2}$ doublets of the metal atoms. Table 1 compares the observations for Ga, In, and Tl. For Ga, solid H_2 blue shifts both components by 210 or 220 ± 20 cm^{-1}, and solid D_2 blue shifts both components by 590 or 600 ± 20 cm^{-1}. Similarly, for In, solid H_2 blue shifts the $^2P_{1/2}$ component 310 ± 20 cm^{-1} and the $^2P_{3/2}$ component 320 ± 20 cm^{-1}, and solid D_2 blue shifts these bands 750 and 760 ± 20 cm^{-1}. However, for Tl, the lower energy $^2P_{3/2}$ emission is blue-shifted more, 315 and 775 ± 20 cm^{-1}, respectively, by solid H_2 and D_2, than the higher energy $^2P_{1/2}$ componentless, namely 210 and 660 ±

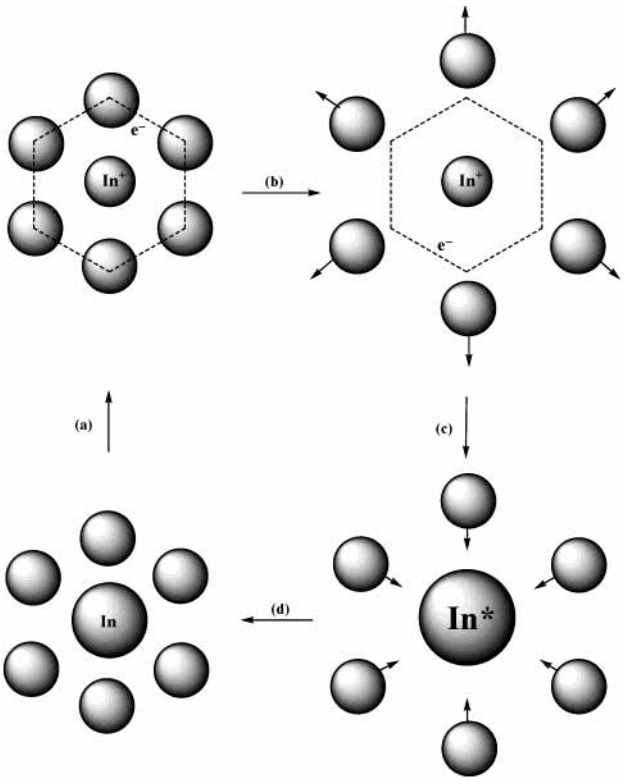

Figure 5. Schematic representation of the hydrogen matrix experiment with atomic indium: (a) Rydberg excitation at 193 nm, (b) cage expansion, (c) initial electronic relaxation, and (d) cage collapse and resonance emission.

20 cm^{-1}. The latter also reveals that the spin−orbit splitting in the ground state,[31] 7793 cm^{-1}, is decreased to 7690 ± 20 cm^{-1} in solid H_2 and to 7680 ± 20 cm^{-1} in solid D_2. Spin−orbit splitting is often altered by the matrix,[34−37] and these small decreases (1.4−1.9%) for solid H_2 and D_2 are reasonable.

The analogous emission for In is red-shifted in solid Kr and Xe,[38] and it is surprising that this emission is blue-shifted in the less polarizable but reactive solid molecular hydrogens, particularly in view of the lack of a shift for the analogous emission of B in solid H_2.[25] How does the "electron bubble" model employed previously[19−21,25] apply to the Ga, In, and Tl cases? The blue shifts observed for the atomic absorptions[33,39] arise from a repulsive metal atom interaction with the matrix cage. See the work of Gruen et al., for example.[40] This leads to a cage expansion as discussed by Chergui and co-workers[21] and shown in Figure 5(a, b) for excitation of Ga, In, and Tl in the region near ionization. What is different here is that apparently Rydberg relaxation, cage collapse, and resonance emission follow more closely for Ga, In, and Tl than for the first-row subjects, which retain small blue shifts for these metals from the gas-phase line positions. Cage collapse probably does not happen for the initial relaxation, Figure 5(c), but is likely associated with the resonance emission, Figure 5(d), observed here. We note that cage expansion is much faster for solid H_2 than D_2 for the NO system,[21] which may imply a greater repulsion for solid D_2 and is in line with our greater observed blue shifts in solid D_2. Table 2 collects atomic properties of the Group 13 atoms—one immediately notices that the metal atoms are much larger than B and senses that the larger metal atoms will interact more strongly with the hydrogen molecule cage, particularly at the stage of the final resonance emission. The excited metal atoms are extremely reactive toward H_2 as the IR spectra of metal hydride products attest,[26−29] which leads to MH* and H in a large fraction of the photophysical events.

TABLE 2: Physical Properties of Group 13 Atoms[a]

atom	radius[b]	IE[c]
B	0.88	801
Al	1.43	578
Ga	1.22	579
In	1.63	558
Tl	1.70	589

[a] Oxtoby, D. W.; Nachtrieb, N. H.; Freeman, W. A. *Chemistry: Science of Change*; Saunders College Pub.: Philadelphia, 1990. [b] Atomic radius in Å (or 10^{-8} cm). [c] First ionization energy in kJ/mol.

In contrast the red-shifted emission for In in solid Kr and Xe[38] is due to their larger internuclear distances (4.00 and 4.33 Å)[41] compared to hydrogen (3.769 Å)[42] and the lack of a reactive interaction with the rare gases.

It is also interesting to note that the resonance emission is blue-shifted more by solid D_2 than solid H_2, namely 380, 440, and 450 ± 20 cm^{-1}, respectively, in the Ga, In, and Tl cases. A similar result has been found for Cu, Ag, and Au atoms: absorption spectra are blue-shifted approximately 240 cm^{-1} more in solid D_2 than in solid H_2.[34] These workers also discuss the repulsive metal atom reaction with the solid molecular hydrogen matrix cage, which is substantially higher in H_2 and D_2 than in the monatomic noble gases.

Normal H_2 and D_2 are both mixtures of ortho and para nuclear spin isomers,[1] but the lattice parameter for solid D_2 (3.600 Å) is smaller than for solid H_2 (3.769 Å).[42,43] Hence, the 4.5% smaller intermolecular distance in solid D_2 suggests a more repulsive cage interaction of the larger radially extending excited atomic state with solid D_2 than with solid H_2, and this is manifested with larger blue shifts in solid D_2 than in solid H_2. This suggests that the even softer and larger (3.789 Å)[1] p-H_2 host would blue shift the atomic emissions slightly less than *n*-H_2. Our measurement for the strongest In emission at 445.5 nm in *p*-H_2 is consistent with this suggestion, as are like observations in *o*-D_2, but our measurements are not accurate enough to confirm this point. We believe that higher resolution measurements in solid *p*-H_2 will find slightly less blue-shifted atomic emissions than solid *n*-H_2.

Metal Atom Reactivity in Solid H_2. No atomic emission signal is detected for Al in solid H_2. Weak emission is observed for Ga in H_2, but stronger atomic emissions are recorded for In and Tl. The chemical reactivities of this group metals play a role here. For Al, all excited Al* atoms react with H_2 giving AlH, AlH_2, and AlH_3. However, for Tl, many of the excited Tl* atoms relax to the $^2S_{1/2}$ state through nonradiative energy transfer and then give strong atomic emission.

Gallium Hydride. The strong 288 (286) nm emissions from the Ga and $H_2(D_2)$ systems disappear on annealing so they appear to be due to a gallium hydride transient species. No emission spectra have been reported for $GaH_{1,2,3}$ species in this region, but these UV emissions are likely due to an unidentified gallium hydride transient species.

InH and InD Emissions. Excited states of InH have been characterized in the visible region ($^1\Pi \rightarrow {}^1\Sigma^+$, 22 655 cm^{-1} and $^3\Pi(0^+) \rightarrow {}^1\Sigma^+$, 16 278 cm^{-1}) but not in the ultraviolet near 193 nm.[44−46] Then how is excited InH formed in these experiments by 193 nm (6.42 eV) radiation? Excited In* reacts with H_2 to form excited InH* which may contain up to 4.42 eV of excess energy since reaction 1 of In and H_2 is 2.0 eV endothermic,[46] and the excess energy of reaction 2 is more than enough to access the $^1\Pi$ and $^3\Pi$ states of InH. Apparently, the solid molecular hydrogens relax InH* to the $^3\Pi$ state 0^+ spin−orbit component before emission occurs. The excellent agree-

ment with the gas phase $^3\Pi(0^+) \rightarrow {}^1\Sigma^+$ emission origin suggests a like assignment for the red matrix phosphorescence.

$$In + H_2 \rightarrow InH + H \quad (\Delta E = +2.0\ eV) \qquad (1)$$

$$In + H_2 + h\nu\ (6.42\ eV) \rightarrow InH + H + E\ (4.42\ eV) \qquad (2)$$

Figure 3 compares the 193 nm excited emissions of InH in solid H_2 and InD in solid D_2 under conditions with comparable In atomic emission intensities and infrared absorbances of InH and InD.[28] Hence, the concentrations of InH* and InD* are likely to be comparable as well. We do find a preference in the reaction of In* with H_2 over D_2 by about 2 to 1 (based on 0.39 absorbance for InH and 0.12 absorbance for InD in a 50/50 H_2/D_2 experiment using the calculated[28] infrared 2:1 intensity), but the InD emission is at least 20× stronger than the InH emission.

Recent ab-initio calculations on InH states show a decrease in frequencies for the $^3\Pi(O^+)$ states of InH and InD relative to the $^1\Sigma^+$ states, respectively,[47] which indicates a small blue deuterium shift in the gas phase. Hence the observed red shift in solid D_2 likely arises from the variation of phonon bands in the different solid molecular hydrogens.

The similar isotopic pair NH and ND have been investigated by fluorescence techniques in rare gas matrixes.[48] The radiative lifetimes of NH and ND are the same within experimental error in solid neon although they are about 75% of the gas-phase value and the band origin is just 22 cm^{-1} higher energy for ND than for NH in solid neon. Hence, we conclude that the lifetimes of InH* and InD* are nearly the same in the gas phase. Since the atomic emission intensities are about the same in the two matrixes, it is likely that the yields of InH* and InD* are also comparable.

We are led to attribute the major difference in InH and InD phosphorescence intensities to the host matrix. We believe that the greater zero-point amplitude of H_2 (18% of the lattice constant) as compared to D_2 (14% of the lattice constant)[1] may be responsible for greater nonradiative relaxation and hence weaker emission for InH in solid H_2. It has also been observed that XeH emission in solid H_2 is a factor of 4 lower than for XeD in solid D_2 following electron irradiation.[17] We note that excited lanthanide ions decay faster in H_2O than in D_2O due to radiationless decay by energy transfer to OH vibrational modes.[49] Again the different solid molecular hydrogen host lattice appears to play a role in the emission process.

Conclusions

Infrared spectra of solid hydrogen (deuterium) samples co-deposited at 3.5 K with laser-ablated Al, Ga, In, and Tl atoms reveal infrared absorptions for the MH [MD] molecules with decreasing intensities, respectively. Irradiation at 193 nm increases MH_2 and MH_3 [MD_2 and MD_3] absorptions and produces emission spectra for the metal atoms, except for Al, and phosphorescence spectra for the InH [InD] molecules. Unreacted metal atomic emission intensities (Ga < In < Tl) follow decreasing metal reactivity with H_2 and are blue-shifted from gas-phase lines more by solid D_2 than by solid H_2. The greater repulsive interaction for D_2 likely arises from the 4.5% smaller lattice parameter for solid D_2. However, the emission yield for InD is much higher in solid D_2 than for InH in solid H_2, which suggests a higher nonradiative relaxation rate in solid H_2 than in solid D_2 owing to the larger zero-point motion in the host solids. The phosphorescence lifetime for the $^3\Pi\ (0^+) \rightarrow {}^1\Sigma$ emission of InD in solid D_2 is estimated as 0.1 s.

The blue-shifted emissions observed here in solid H_2 and D_2 are unique to these large, reactive guest atoms, as the resonance emission of B in solid H_2 is unshifted from the gas-phase position.[25] The matrix cage apparently relaxes with the excited metal atoms, resulting in blue shifts.

Acknowledgment. We gratefully acknowledge support for this work from N.S.F Grant CHE 00-78836, loan of the Ocean Optics spectrometer system by J. C. Zieman, and very helpful referee suggestions.

References and Notes

(1) Silvera, I. F. *Rev. Mod. Phys.* **1980**, *52*, 393.
(2) Weltner, W., Jr.; Van Zee, R. J.; Li, S. *J. Phys. Chem.* **1995**, *99*, 6277.
(3) Van Zee, R. J.; Li, S.; Weltner, W., Jr. *J. Chem. Phys.* **1995**, *102*, 4367.
(4) (a) Fajardo, M. E., Tam, S. *J. Chem. Phys.* **1998**, *108*, 4237. (b) Tam, S.; Macler, M.; Fajardo, M. E. *J. Chem. Phys.* **1997**, *106*, 8955.
(5) Momose, T.; Shida, T. *Bull. Chem. Soc. Jpn.* **1998**, *71*, 1.
(6) Andrews, L.; Wang, X. *Science* **2003**, *299*, 2049.
(7) Wang, X.; Andrews; L.; Tam, S.; DeRose, M. E.; Fajardo, M. E. *J. Am. Chem. Soc.* **2003**, *125*, 9218 (Al + H_2).
(8) Wang, X.; Andrews, L. *J. Am. Chem. Soc.* **2003**, *125*, 6581 (Pb + H_2).
(9) Wang, X.; Andrews, L. *J. Phys. Chem. A* **2003**, *107*, 570 (Cr + H_2).
(10) Wang, X.; Souter, P. F.; Andrews, L. *J. Phys. Chem. A* **2003**, *107*, 4244 (Bi + H_2).
(11) Wang, X.; Andrews, L. *J. Phys. Chem. A* **2002**, *106*, 3706 (Rh + H_2).
(12) Andrews, L.; Wang, X. *J. Am. Chem. Soc.* **2003**, *125*, 11751 (AuH_2^-).
(13) Wang, X.; Andrews, L. *J. Phys. Chem. A* **2004**, *108*, 1103 (H^- in H_2).
(14) Gruen, D. M.; Bates, J. K. *Inorg. Chem.* **1977**, *16*, 2450.
(15) Harris, A. B.; Meyer, H.; Qin, X. *Phys. Rev. B* **1994**, *49*, 3844.
(16) Brooks, R. L. *J. Chem. Phys.* **1986**, *85*, 1247.
(17) Schou, J.; Stenum, B.; Sørensen; Gürtler, P. *Phys. Rev. Lett.* **1989**, *63*, 969.
(18) Magnotta, F.; Collins, G. W.; Mapoles, E. R. *Phys. Rev. B* **1994**, *49*, 11817.
(19) Jeannin, C.; Portella-Oberli, M. T.; Viglietti, F.; Chergui, M. *Chem. Phys. Lett.* **1997**, *279* (1), 65.
(20) Vigliotti, F.; Cavina, A.; Bressler, Ch.; Lang, B.; Chergui, M. *J. Chem. Phys.* **2002**, *116*, 4542, and references therein.
(21) Vigliotti, F.; Bonacina, L.; Chergui, M. *J. Chem. Phys.* **2002**, *116*, 4553.
(22) Danilychev, A. V.; Bondybey, V. E.; Apkarian, V. A.; Tanaka, S.; Kajihara, H.; Koda, S. *J. Chem. Phys.* **1995**, *103*, 4292.
(23) Danilychev, A. V.; Apkarian, V. A.; Kajihara, H.; Tanaka, S.; Koda, S. *Low Temp. Phys.* **2000**, *26*, 669.
(24) Fajardo, M. E.; Tam, S.; Thompson, T. L.; Cordonnier, M. E. *Chem. Phys.* **1994**, *189*, 351.
(25) Tam, S.; Macler, M.; DeRose, M. E.; Fajardo, M. E. *J. Chem. Phys.* **2000**, *113*, 9067.
(26) Wang, X.; Andrews, L. *J. Phys. Chem A*, **2004**, *108*, 4202 (Al + H_2).
(27) Wang, X.; Andrews, L. *J. Phys. Chem. A* **2003**, *107*, 11371 (Ga + H_2).
(28) Wang, X.; Andrews, L. *J. Phys. Chem. A* **2004**, *108*, 4440 (In + H_2).
(29) Wang, X.; Andrews, L. *J. Phys. Chem A* **2004**, *108*, 3396 (Tl + H_2).
(30) Andrews, L.; Citra, A. *Chem. Rev.* **2002**, *102*, 885.
(31) Moore, C. E. *Atomic Energy Levels*; Circular 467, National Bureau of Standards: Washington, DC, 1952.
(32) CRC Handbook, Line Spectra of the Elements, 66th ed.; CRC Press: Boca Raton, FL, 1985.
(33) Schroeder, W.; Rotermund, H.-H.; Wiggenhauser, H.; Schrittenlacher, W.; Hormes, J.; Krebs, W.; Laaser, W. *Chem. Phys.* **1986**, *104*, 435.
(34) Abe, H.; Schulze, W.; Kolb, D. M. *Chem. Phys. Lett.* **1979**, *60*, 208, and references therein.
(35) Vala, M.; Zerlinque, K.; ShakhsEmampour, J.; Rivoal, J.-C.; Pyzalski, R. *J. Chem. Phys.* **1984**, *80*, 2401.
(36) Rose, J.; Smith, D.; Williamson, B. E.; Schatz, P. N.; O'Brien, M. C. M. *J. Phys. Chem.* **1986**, *90*, 2608.
(37) Pellow, R.; Vala, M. J. *J. Chem. Phys.* **1989**, *90*, 5612.
(38) Balling, L. C.; Wright, J. J. *J. Chem. Phys.* **1981**, *74*, 6554.

(39) Ammeter, J. H.; Schlosnagle, D. C. *J. Chem. Phys.* **1973**, *59*, 4748.
(40) (a) Gruen, D. M.; Gaudioso, S. L.; McBeth, R. L.; Lerner, J. L. *J. Chem. Phys.* **1974**, *60*, 89. (b) Gruen, D. M.; Bates, J. K. *Inorg. Chem.* **1977**, *16*, 2450.
(41) Pollack, G. L. *Rev. Mod. Phys.* **1964**, *36*, 748.
(42) Krupskii, I. N.; Prokhvatilov, A. I.; Shcherbakov, G. N. *Sov. J. Low Temp. Phys.* **1983**, *9*, 446.
(43) Shcherbakov, G. N. *Sov. J. Low Temp. Phys.* **1991**, *17*, 73.
(44) Ginter, M. L. *J. Mol. Spectrosc.* **1963**, *11*, 301.
(45) Ginter, M. L. *J. Mol. Spectrosc.* **1966**, *20*, 240.
(46) Huber, K. P.; Herzberg, G. *Constants of Diatomic Molecules*; Van Nostrand: Princeton, 1979.
(47) Zou, W.; Lin, M.; Yang, X.; Zhang, B. *Phys. Chem. Chem. Phys.* **2003**, *5*, 1106.
(48) Bondybey, V. E.; Brus, L. E. *J. Chem. Phys.* **1975**, *63*, 794.
(49) Horrocks, W. DeW., Jr.; Sudnik, D. R. *J. Am. Chem. Soc.* **1979**, *101*, 334.